1 Comparison with another RWB detection algorithm

We have initially used a RWB detection algorithm similar to the one used in Ndarana and Waugh (2010) and Garfinkel and Waugh (2014), which give very similar results. As can be seen in Fig. S1 and Fig. S2, which are equivalent to Fig 2 and Fig. 3 of the manuscript but based on the former RWB detection algorithm, both methods yield very similar results (this holds true for all the other results found in this study). However, we found extensive and unexpected CWB activity in the region where AWB is most frequent (Fig. S3), which is not consistent with other studies. Since we were not able to identify the reason for this spurious CWB activity, we decided to switch to an alternative algorithm. Nonetheless, the similarity of the results using the two different RWB detection methods gives confidence in our results.

Note that the RWB we initially used, presented here, detects the breaking events at a slightly earlier (less developed) stage (compare Fig. S1 with Fig. 2 of the manuscript). Hence, it highlights more strongly the tilt of the positive-negative-positive vorticity anomalies during AWB (i.e., that one cyclonic anomaly is to the NW and one is to the SE of the anticyclonic vorticity). Similarly, it shows more clearly the tilt of the positive-negative vorticity anomalies during CWB (i.e., that the anticyclonic anomaly is to the SE of the cyclonic vorticity). This is also more evident in the relative cyclone and anticyclone positions, shown in Fig. S2.
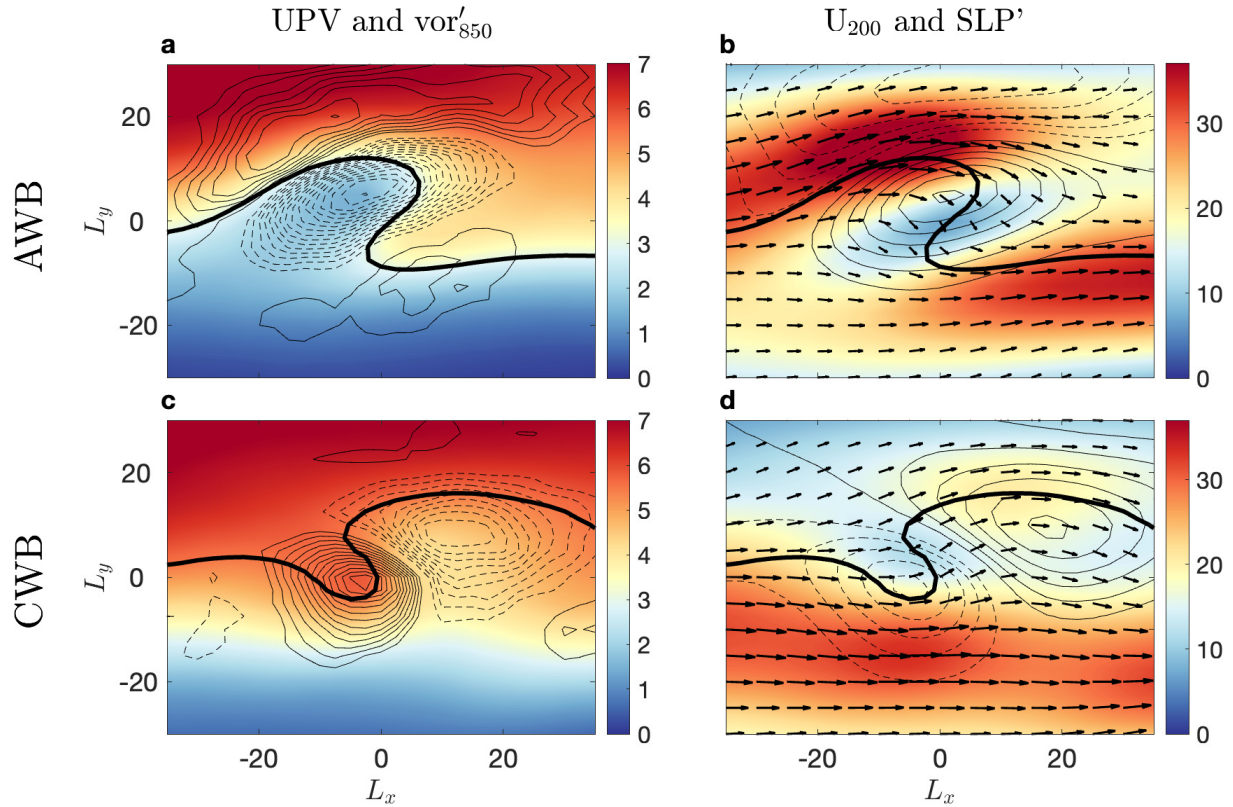
Figure S1: As in Fig. 2 of the manuscript, but based on a RWB detection algorithm similar to the one used in Ndarana and Waugh (2010) and Garfinkel and Waugh (2014).
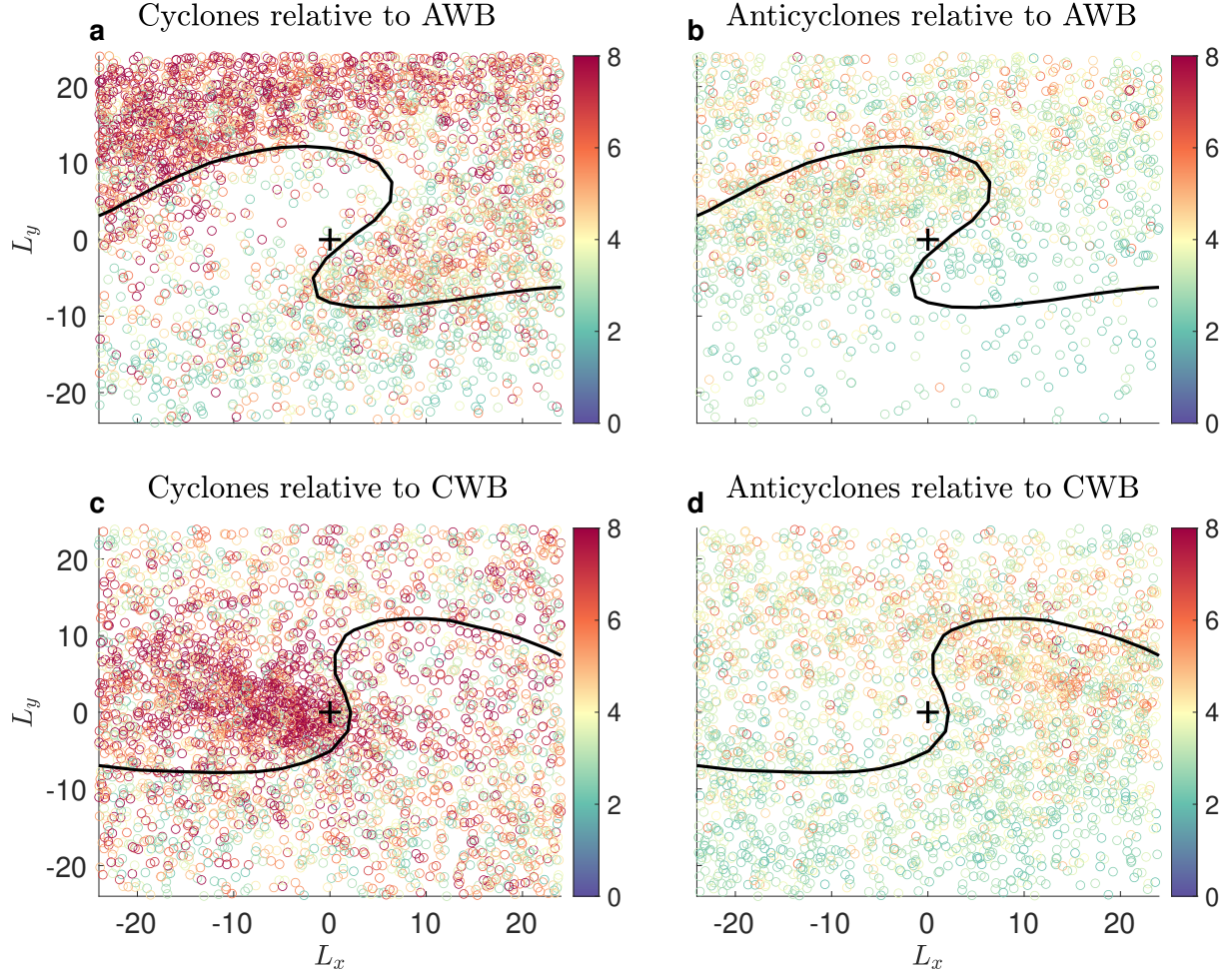
Figure S2: As in Fig. 3 of the manuscript, but based on a RWB detection algorithm similar to the one used in Ndarana and Waugh (2010) and Garfinkel and Waugh (2014).
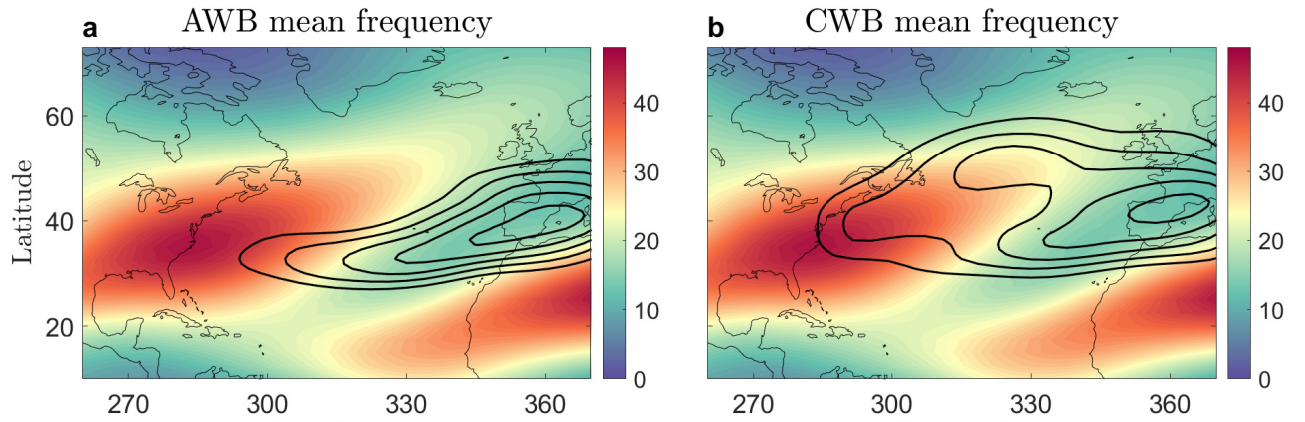
Figure S3: As in Fig. 1c,d of the manuscript, but based on a RWB detection algorithm similar to the one used in Ndarana and Waugh (2010) and Garfinkel and Waugh (2014).

2 Life-cycle of anticyclones and cyclones in the North Atlantic

Fig. S4 and Fig. S5 show composites of 1,750 anticyclones and cyclones, respectively, calculated by taking the strongest 50 storms from each year, for 35 years from 1980-2014, based on ERAI reanalysis data. For the compositing, only storms whose maximum intensity was achieved in the Atlantic domain (30N-60N and 80W-20E) are kept for the analysis. The T=0 timestep denotes the time of storm's maximum intensity (based on the 850 hPa vorticity). For other time-steps, the time-lagged composites may involve averaging over a smaller number of storms, since not all storms have a large enough lifetime.
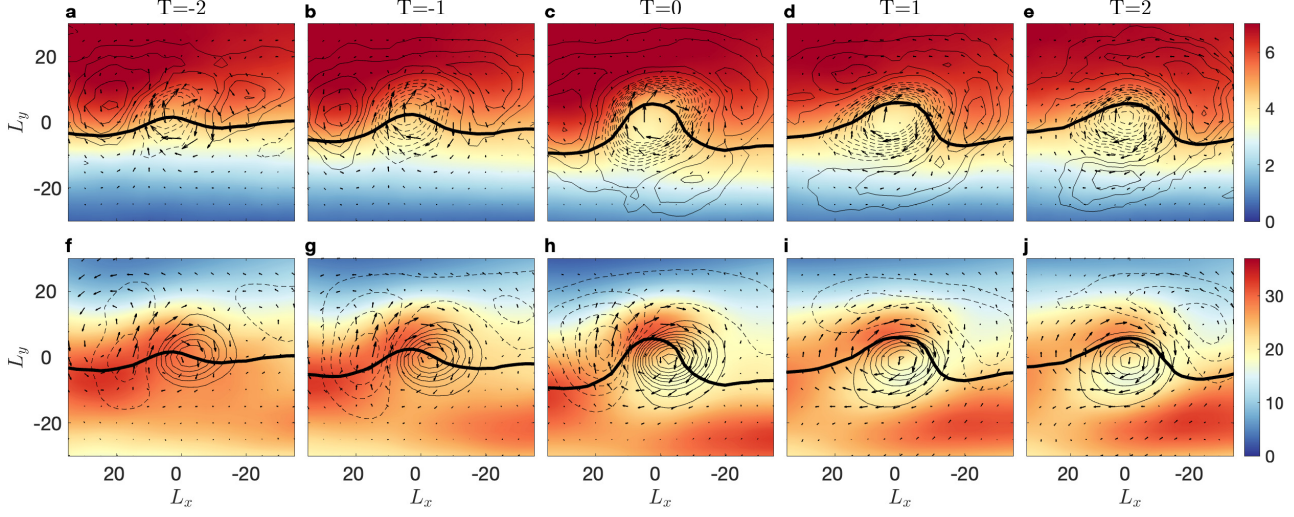
Figure S4: Composites centered around anticyclones, showing the life-cycle of anticyclones in the North-Atlantic region (30N-60N and 80W-20E), from two days prior to the maximum intensity ($T = -2$), and up to two days after the maximum intensity ($T = 2$). Panels (a-e) show the upper-level (250 hPa) PV (colors) and the PV anomaly (in PVU), while the arrows denote the anomalous low-level (850 hPa) velocities. Panels (f-j) show the upper-level (250 hPa) zonal velocity (in ms^{-1}) and the SLP anomaly (in mb), and the arrows show the anomalous upper-level (250 hPa) velocities. L_y and L_x denote the relative latitudinal and longitudinal distance (in degrees), respectively, from the center of the anticyclones. In all panels, the black line denotes the 4.5 PVU contour.
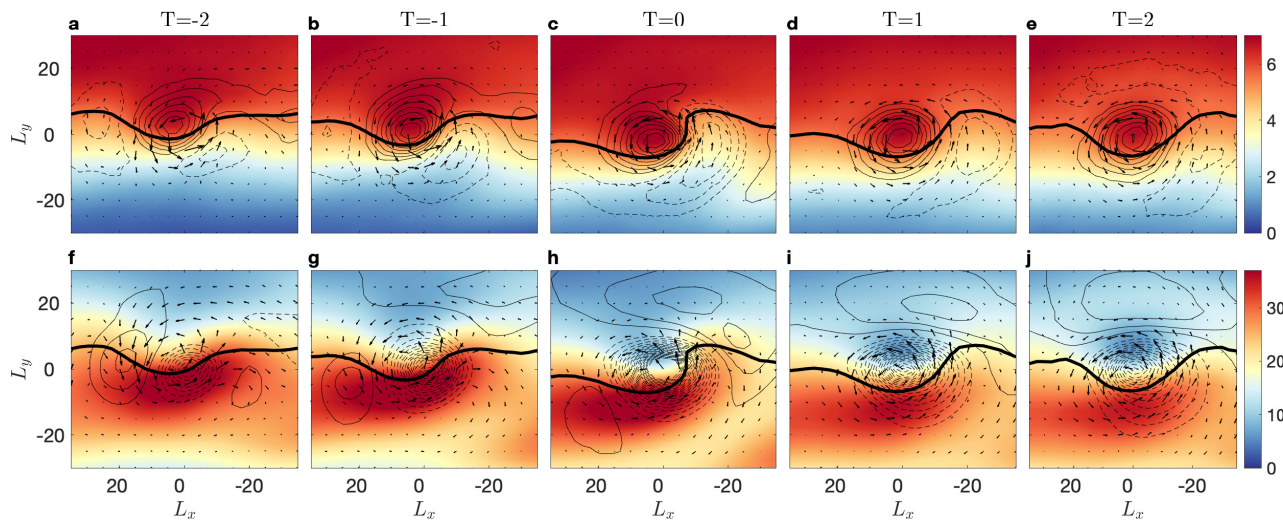
Figure S5: Same as in Fig. S1, but for composites centered around cyclones, showing the life-cycle of cyclones in the North-Atlantic region. In all panels, the black line denotes the 5.5 PVU contour.

3 Composites of upper level time-averaged and anomalous flow

Fig. S6 and Fig. S7 show the upper level (250 hPa) time averaged zonal velocity (first row) and anomalous zonal (second row) and meridional (third row) velocities, for the same anticyclones during AWB and cyclones during CWB shown in Fig. 6 and Fig. 8 of the manuscript.
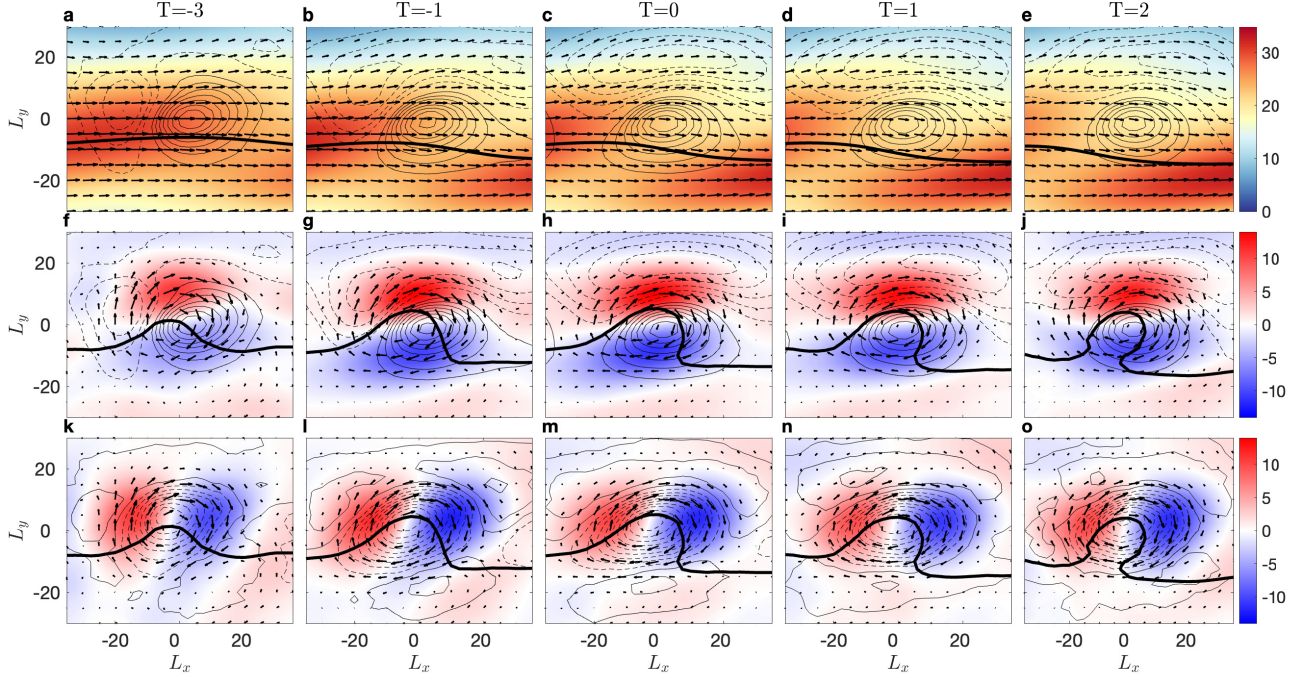
Figure S6: Composites centered around anticyclones during AWB events, showing the time evolution of AWB in the North-Atlantic region, from two days prior to the breaking ($T = -2$), and up to two days after the breaking ($T = 2$). Shown are the upper-level (250 hPa) time-averaged zonal velocity (colors) in ms^{-1} and the SLP anomaly in mb (contours) (first row), the upper-level anomalous zonal velocity (colors) in ms^{-1} and SLP anomaly (contours) (second row), and the upper-level anomalous meridional velocity (colors) in ms^{-1} and upper-level PV anomaly (contours) (third row). The arrows in panels a-e show the time-averaged upper-level velocities, while in panels f-o the anomalous upper-level velocities are shown. L_y and L_x denote the relative latitudinal and longitudinal distance (in degrees), respectively, from the center of the breaking. In all panels, the black line denotes the 3.2 PVU contour.
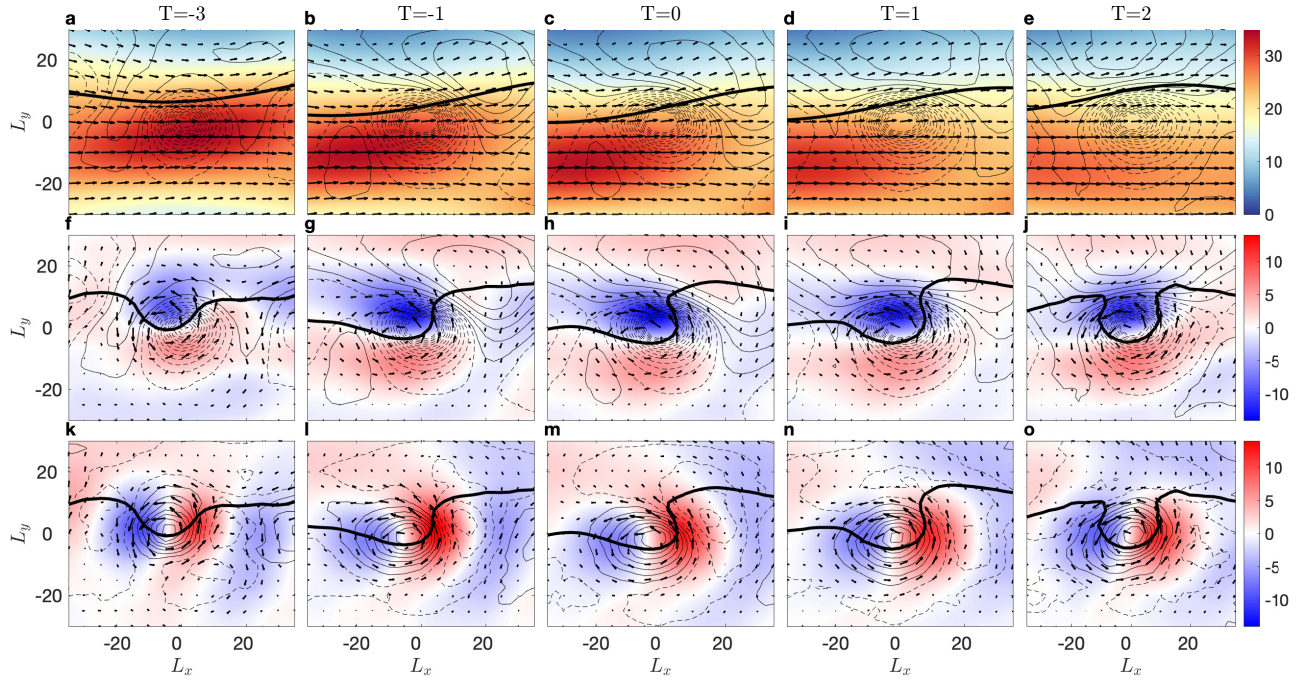
Figure S7: Same as Fig. S3, but for composites centered around cyclones during CWB events, showing the time evolution of CWB in the North-Atlantic region. In all panels, the black line denotes the 5.8 PVU contour.

4 Cross sections of upper-level U fixed by latitudinal displacement

The results presented in Fig. 7 in the manuscript are calculated using composites centered around the anticyclones (for AWB) and the cyclones (for CWB), which are propagating meridionally. Hence, in order to consider how the upper-level zonal flow changes from a fixed reference point, the cross sections are corrected to account for this by adding the averaged latitudinal displacement of the anticyclones or cyclones at each time-step. This shows that while the peak of upper-level U is shifted poleward during the time-evolution of AWB events, it remains roughly at the same latitude for CWB events.
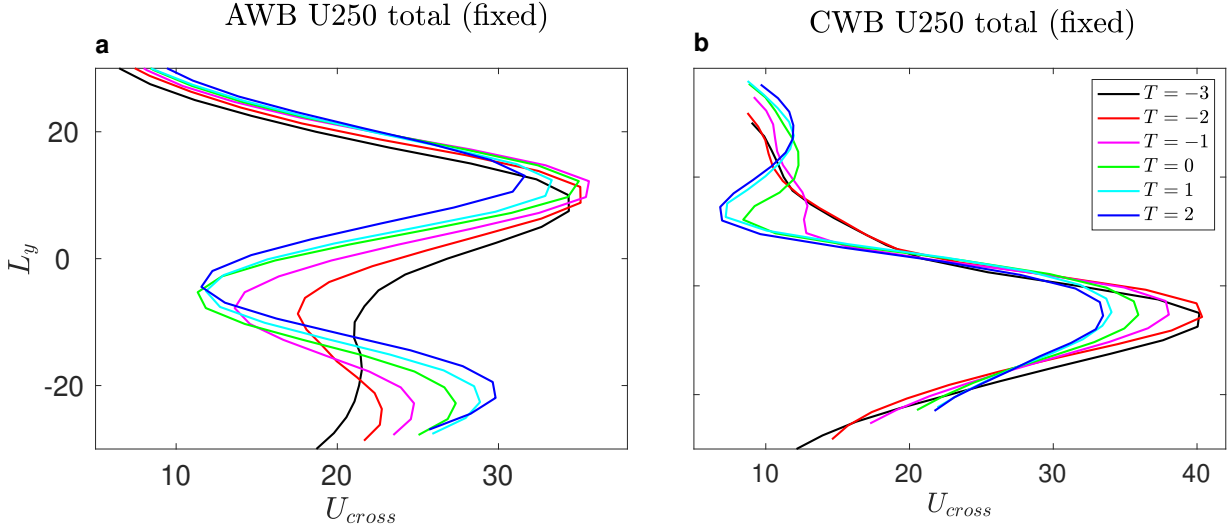
Figure S8: Corrected cross sections of the composite upper-level (250 hPa) total zonal velocity (in units of ms^{-1}), at the longitude crossing the center of (a) anticyclones during AWB events, and (b) cyclones during CWB events. The cross-sections are corrected by adding the averaged latitudinal displacement of the anticyclones (for AWB events) or cyclones (for CWB events) at each time-step, where $T = -3$ is chosen as the starting point, and all the other time-steps are then shifted according to the averaged latitudinal displacement of the storms from $T = -3$. The colors indicate the time, going from black (three days prior to the breaking), to blue (two days after to the breaking). L_y is the corrected relative latitudinal distance (in degrees) from the center of the anticyclones (for AWB) and the cyclones (for CWB).